ELSEVIER

Global and Planetary Change 25 (2000) 133–147

GLOBAL AND PLANETARY CHANGE

www.elsevier.com/locate/gloplacha

Evaporation from groundwater discharge playas, Estancia Basin, central New Mexico

Kirsten M. Menking [a,*], Roger Y. Anderson [b], Nathaniel A. Brunsell [b], Bruce D. Allen [c], Amy L. Ellwein [b], Thomas A. Loveland [b], Steven W. Hostetler [d]

[a] *Department of Geology and Geography, Vassar College, 124 Raymond Avenue, Poughkeepsie, NY 12604, USA*
[b] *Department of Earth and Planetary Sciences, Northrup Hall, University of New Mexico, Albuquerque, NM 87131, USA*
[c] *New Mexico Bureau of Mines, New Mexico Institute of Mining and Technology, Socorro, NM 87801, USA*
[d] *US Geological Survey, 200 SW 35th St., Corvallis, OR 97333, USA*

Received 22 October 1998; accepted 16 August 1999

Abstract

Bowen ratio meteorological stations have been deployed to measure rates of evaporation from groundwater discharge playas and from an adjacent vegetated bench in the Estancia Basin, in central New Mexico. The playas are remnants of late Pleistocene pluvial Lake Estancia and are discharge areas for groundwater originating as precipitation in the adjacent Manzano Mts. They also accumulate water during local precipitation events. Evaporation is calculated from measured values of net radiation, soil heat flux, atmospheric temperature, and relative humidity. Evaporation rates are strongly dependent on the presence or absence of standing water in the playas, with rates increasing more than 600% after individual rainstorms. Evaporation at site E-12, in the southeastern part of the playa complex, measured 74 cm over a yearlong period from mid-1997 through mid-1998. This value compares favorably to earlier estimates from northern Estancia playas, but is nearly three times greater than evaporation at a similar playa in western Utah. Differences in geographical position, salt crust composition, and physical properties may explain some of the difference in evaporation rates in these two geographic regions.

Keywords: Estancia Basin; Bowen ratio; evaporation; playa; meteorological station

1. Introduction

Potentially important records of past changes in hydrology and climate exist in sediments that have accumulated beneath lakes in ‘‘closed’’ basins, where lake surface area and water level have been responsive to changes in climate. If a lake is still present in a basin, meteorological and hydrological data (e.g. evaporation) from the lake and the basin can be used to develop and validate basin models, which help provide an understanding of the modern hydrologic system and facilitate interpretation of the sedimentary record (e.g. Hostetler and Bartlein, 1990; Hostetler and Benson, 1994). Some highly respon-

* Corresponding author. Tel.: +1-914-437-5545; fax: +1-914-437-7577.
E-mail address: kimenking@vassar.edu (K.M. Menking).

0921-8181/00/$ - see front matter
PII: S0921-8181(00)00025-4

sive lake-sediment records, however, are found in basins in which previously expanded lakes are nearly desiccated and which instead contain ephemeral lakes or playas. In such settings, it may still be possible to estimate rates of evaporation and develop basin models to quantitatively estimate past hydrologic and climatic changes recorded in the basin.

Although there have been many studies of evaporation from lakes, measurements of evaporation from playas are scarce (Malek et al., 1990). Here, we report on investigations of evaporation from a large playa complex in the Estancia Basin in central New Mexico (Fig. 1). During the late Pleistocene and the beginning of the Holocene, the basin contained a large (400 to 1100 km^2) perennial lake alternatively fed by groundwater discharge or by a combination of groundwater and surface flow from the Manzano Mts. to the west (Allen and Anderson, 1993; Bachhuber, 1971). In the mid-Holocene, however, the lake desiccated and more than 80 deflation basins (playas) developed coincident with a lowering of the water table by as much as 10 m below the old lake floor; each playa has an associated lunette formed from the deflated lake bed sediments (Fig. 1). Thereafter, the water table rose, allowing the deflation basins to collect 20 to 170 cm of sediment derived from fluvial erosion of the lunettes and aeolian transport.

The atmospheric and hydrologic conditions that led to the desiccation of Lake Estancia during the mid-Holocene as well as the precipitation–evaporation balance that allowed the lake to reach its

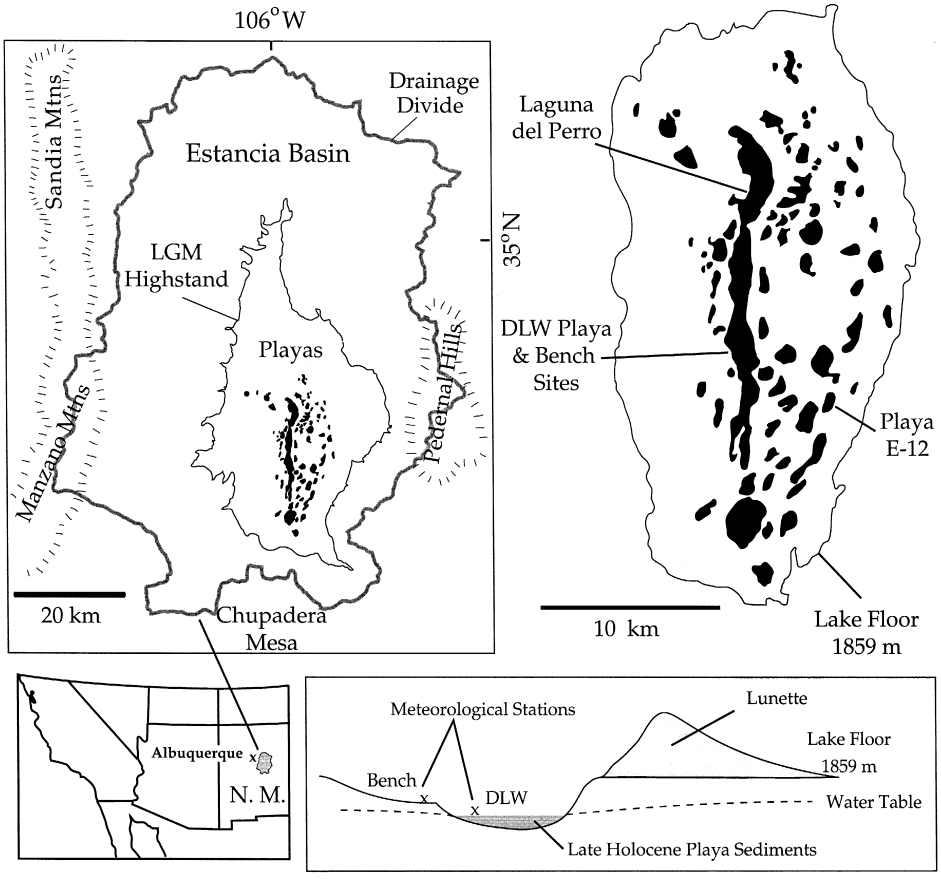

Fig. 1. Map of the Estancia Basin showing location of highstand shoreline, Estancia playa complex, and meteorological stations at the Laguna del Perro and E-12 playas. Also depicted is a diagrammatic cross-section of a typical playa showing the erosional bench, playa lake, and lunette, and the relative locations of the meteorological stations at Laguna del Perro (DLW and BENCH).

highstand level during the Last Glacial Maximum are unknown. To estimate the hydrologic balance at those times requires an understanding of the modern relationship between climatic variables and water table fluctuations. Toward that end, we have installed three meteorological stations on the deflation basins and a nearby vegetated bench above one of the playas. We have also installed nests of piezometers across several of the playas to record water table fluctuations, estimate groundwater movement into the playas, and compare meteorological and hydrological estimates of evaporation rates. In this paper, we report the results of the meteorological investigations.

2. Geologic and climatic setting of Estancia Basin

The Estancia basin is located in Torrance County, ~100 km southeast of Albuquerque, in central New Mexico (Fig. 1). The 5000 km^2 drainage area is bordered on the west by the Precambrian and Paleozoic carbonate, clastic, and evaporite rocks of the Sandia, Manzano, and Manzanita Mts., on the east by the Precambrian crystalline rocks of the Pedernal Hills, to the south by the Permian limestones, sandstones, and evaporites of the Chupadera Mesa, and to the north by Mesozoic shales and sands (Allen, 1993; Bachhuber, 1971; DeBrine, 1971).

The interior of the basin contains alluvial fill, which consists of a basal unit of alluvial silts, sands, and gravels, with a maximum thickness greater than 120 m, and an overlying lacustrine unit of silts and clays, measuring slightly more than 30 m maximum thickness (Titus, 1969; DeBrine, 1971). The lacustrine unit near the lake margin consists of two clay packages separated by a fine- to medium-grained sand unit that does not reach the center of the basin (Allen, 1993). The upper part of the clay sequence represents the latest Pleistocene pluvial lake cycle (Titus, 1969; Allen, 1993). Within the upper clay exist occasional layers of gypsum sand, deposited during lower lake stands (Allen, 1993).

The basin experiences a continental climate, with mean monthly temperatures in January and July of 0°C and 21°C, respectively on the valley floor (Tuan et al., 1973). Mean annual precipitation in the basin ranges from 35 cm on the valley floor to more than 75 cm at 3000 m, along the crest of the Manzano Mountains (Tuan et al., 1973; Local Climatological Data (NOAA)). Nearly 60% of the precipitation on the valley floor falls in the summer months when the Arizona monsoon forms over the Southwest, drawing in moist air masses from the Gulfs of Mexico and California and from the Pacific (Hales, 1974). The remaining 40% falls in winter when Pacific cyclones travel inland with the zonal winds (Bryson and Hare, 1974). Along the range crest, the proportions of summer and winter moisture are nearly equivalent (Tuan et al., 1973).

Evaporation in the region ranges from ~112 cm/year at Santa Fe (Leopold, 1951) to ~132 cm/year at Albuquerque (Bachhuber, 1971). Under modern P–E conditions, there is no surface runoff from the subbasins, and water levels within the playas are maintained by groundwater discharge, by precipitation falling directly on the playas, and during summer thunderstorms, by surface flow from slopes adjacent to the playas. Groundwater recharge is mainly from the upper slopes and foothills of the Manzano Mountains, with lesser recharge around the perimeter of the drainage basin. Most of the groundwater contained within the valley fill is supplied by the Pennsylvanian Sandia and Madera Formations, which comprise cherty limestones, shales, arkosic sandstones, and calcarenites, and which slope gently eastward beneath the valley fill from their exposures in the Manzanos (Titus, 1969; DeBrine, 1971).

Vegetation on the valley floor is a mixture of grass and desert shrubs, with halophytes near the margins of playas. Flat areas and slopes above the valley floor are commonly occupied by piñon (*Pinus edulis*) and juniper (*Juniperus monosperma*), with oak (*Quercus gambelii*), pine (*P. ponderosa*), spruce (*Picea engelmanii*) and fir (*Pseudotsuga menziesii*, *Abies lasiocarpa*) along the rangecrest of the Manzanos (Bachhuber, 1971).

3. Estancia playa complex

The blowout basins and area of groundwater discharge are restricted to the flat, desiccated floor of the Pleistocene lake, at an elevation of 1855 m. The deepest blowout is cut ~10 m below the floor of the pluvial lake. The largest, Laguna del Perro,

follows the N–S axis of the basin, is ~19 km long, and covers an area of ~19 km^2 (Fig. 1). The other blowouts are generally <1 km^2 in size and all the blowouts, together, have an area of ~50 km^2. The bottoms of the blowouts are occupied by ephemeral salty lakes (playas).

Piezometers screened in gypsum sand layers within the lacustrine sediments indicate upward-directed groundwater movement within the playas (unpublished data). Piezometers on the playas screened at a depth of ~4 m show higher values of hydraulic head than those screened at shallower depths, indicating that the gypsum sand layers constitute confined aquifers within the lacustrine package. Water levels in piezometers in central and eastern playas show an annual cycle up to ~1 m in amplitude, with highest levels occurring in mid-summer and lowest levels in mid-winter. For example, at playa E-12, water levels in deep piezometers are as much as 1 m above the playa surface in summer. In other areas, as on the western margin of Laguna del Perro, water levels through the year range from ~20 cm above to ~20 cm below the playa surface.

4. Estimates of evaporation

Meteorological estimates of evaporation from the playa complex, as well as estimates of discharge obtained from groundwater flow data, are being made to assess the impact of various meteorological parameters on water table fluctuations under modern conditions. The independent estimates will help calibrate a hydrologic model of Estancia basin presently under construction. The model, which will consist of a MODFLOW (McDonald and Harbaugh, 1988) component to simulate the groundwater flow system, a Soil and Water Assessment Tool (SWAT; Arnold et al., 1995) component to simulate surface water flow and infiltration, and an energy balance model developed by Hostetler (1987) to determine evaporation from lakes, will be used in conjunction with regional climate model simulations of the late Pleistocene and mid-Holocene to determine the atmospheric conditions necessary to create the lake highstands and lowstands recorded in the sedimentologic and geomorphic records. When completed, the model results will be reported elsewhere.

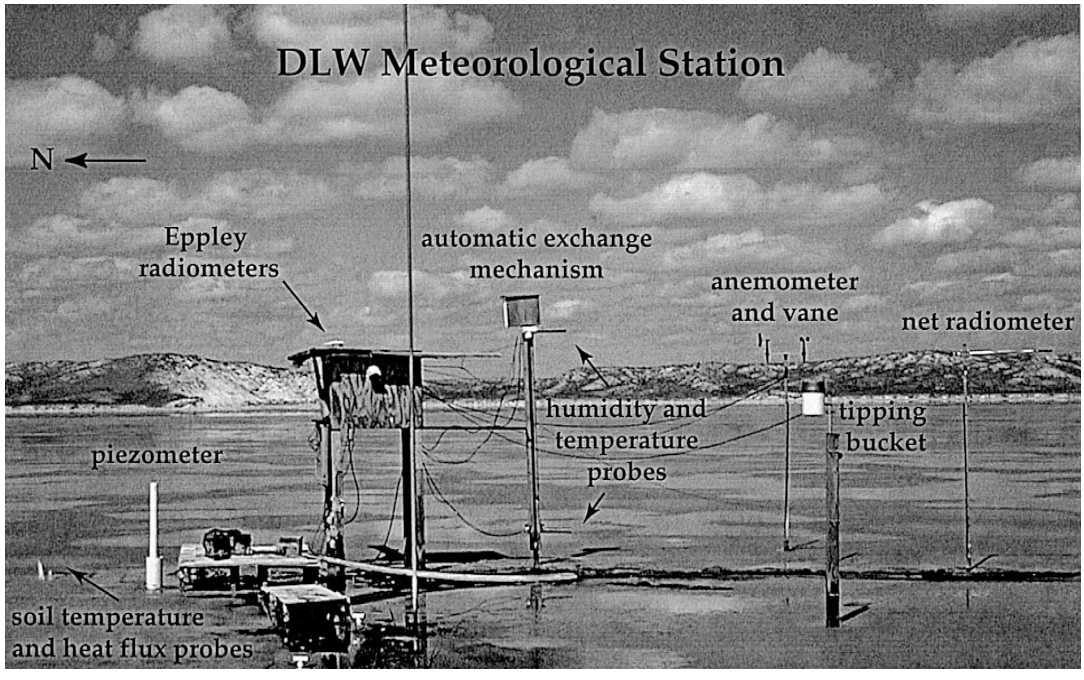

Fig. 2. Photograph of the Laguna del Perro meteorological station (DLW).

In this study, evaporation is estimated using the Bowen ratio (Bowen, 1926), and the meteorological stations used in this study are installed at the Laguna Del Perro and E-12 playas (Fig. 1). The Laguna del Perro station (abbreviated DLW) is located ~75 m east of the western shore of the blow-out in an area of saturated, soft mud covered by a 1–5 cm thick crust of halite and gypsum (Fig. 2). A plywood pier is used for access. The E-12 station (E-12) lies ~50 m west of the eastern shore of the blowout and is surrounded by firm, damp mud. A ring of halite and gypsum salt, less than 1 cm thick and approximately 10 m wide, occasionally forms on the surface of the playa toward its southern end. The meteorological station lies beyond the ring, toward the center of the playa. Both playas often contain standing water up to 15 cm deep, but this water does not dissolve much of the underlying salt crust at DLW. Indeed, in winter, ice has been observed to form in a few centimeters of water directly above the halite layer.

A third meteorological station (BENCH) is located on a grassy surface on a cut bench above and about 150 m west of the playa margin at Laguna del Perro. This station is being used to measure evaporation and evapotranspiration from a vegetated area adjacent to the DLW site. The bench represents an early episode of deflation and is therefore cut into the Pleistocene lakebeds such that the soil in this area is gypsiferous clay. Ground cover on the bench and in the immediate area of the station consists of several species of grass, with areas of bare ground ranging from ~40% to ~70% of the total area, and with the grass canopy generally 20–40 cm above bare ground. Isolated occurrences of four-winged saltbush (*Atriplex canescens*) are within ~30 m of the station.

5. The Bowen ratio method for determining evaporation rates

Evaporation rates are notoriously difficult to constrain (Winter, 1981), particularly for playas. Pan evaporation rates are usually inaccurate, and use of lysimeters difficult. For this reason, evaporation is commonly assessed using an energy balance approach. The energy balance at Earth's surface is written (Oke, 1987; Duell, 1990):

$$R_n - G - H - \lambda E = 0 \quad (1)$$

where R_n = net radiation [W/m^2]; G = soil heat flux [W/m^2]; H = sensible heat flux [W/m^2]; λE = latent heat flux [W/m^2]; λ = latent heat of vaporization [2450 J/g]; E = quantity of water evaporated [g/m^{2}s]. Net radiation (R_n), which is a balance between net solar radiation (incoming shortwave minus outgoing shortwave) and net longwave radiation (incoming longwave minus outgoing longwave), is available to heat soil (G), evaporate water (λE), and warm the air in contact with the surface (H).

The relative importance of the sensible and latent heat fluxes is described by the Bowen ratio, β (Bowen, 1926):

$$\beta = H/\lambda E. \quad (2)$$

This allows the energy balance equation to be recast to solve for the evaporation rate:

$$E = (R_n - G)/(\lambda^*(1+\beta)). \quad (3)$$

The Bowen ratio may be determined from the expression (Brutsaert, 1982; Tomlinson, 1996):

$$\beta = \gamma^*(\Delta T/\Delta e_a) \quad (4)$$

where γ is the pyschrometric constant (dependent on atmospheric pressure, air heat capacity, and the latent heat of vaporization). ΔT and Δe_a are vertical temperature and vapor pressure profiles.

6. Meteorological instrumentation

Bowen ratio stations consist of a Radiation and Energy Balance Systems Q*7 modified Fritschen net radiometer (for determining R_n), two Campbell Scientific, Inc. CS500 temperature/relative humidity probes (for determining ΔT and Δe_a), and a soil heat flux plate either constructed from a Peltier cooler manufactured by MELCOR (after Weaver and Campbell, 1985; for measuring G) or purchased from Radiation and Energy Balance Systems (model HFT-3). Campbell Scientific, Inc. 107B thermometers are located at 2 and 6 cm above the soil heat flux plates, which are buried at a depth of 8 cm; these thermometers are used to assess the amount of heat storage in the soil above the heat flux plates to correct those values in the energy balance equation

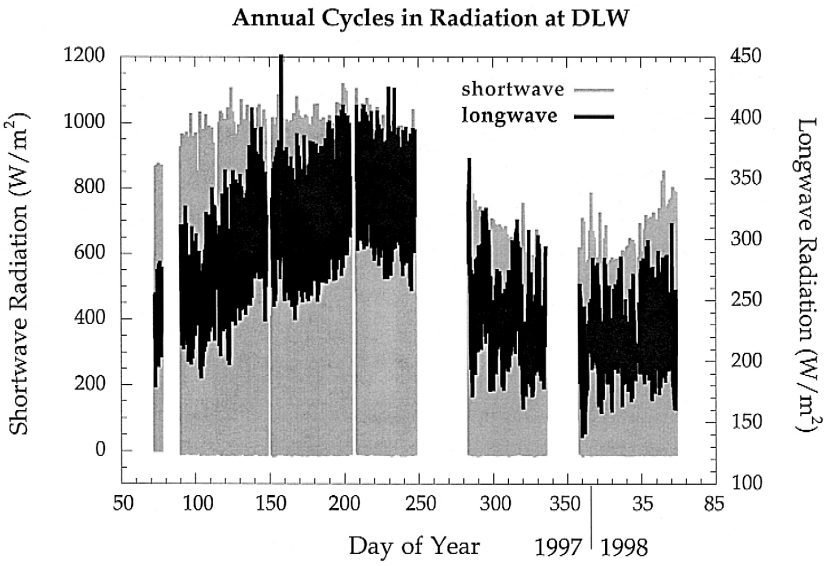

Fig. 3. Incoming short- and long-wave radiation at DLW show a strong annual cycle. Values of shortwave radiation are zero at night whereas longwave radiation continues to be emitted by the atmosphere and by clouds.

(Fuchs and Tanner, 1968; Campbell Scientific, 1997; Tomlinson, 1996). The temperature/relative humidity probes are mounted 2 m apart on an automatic exchange mechanism and the sensors are exchanged every 10 min to eliminate sensor bias. Each station also has a Texas Instruments TE525 tipping bucket rain gage and an R.M. Young Wind Sentry wind vane and anemometer (Campbell Scientific, model number 03001). DLW additionally contains two Eppley precision spectral pyranometers and two Eppley precision infrared radiometers to measure both incoming and outgoing long- and short-wave radiation

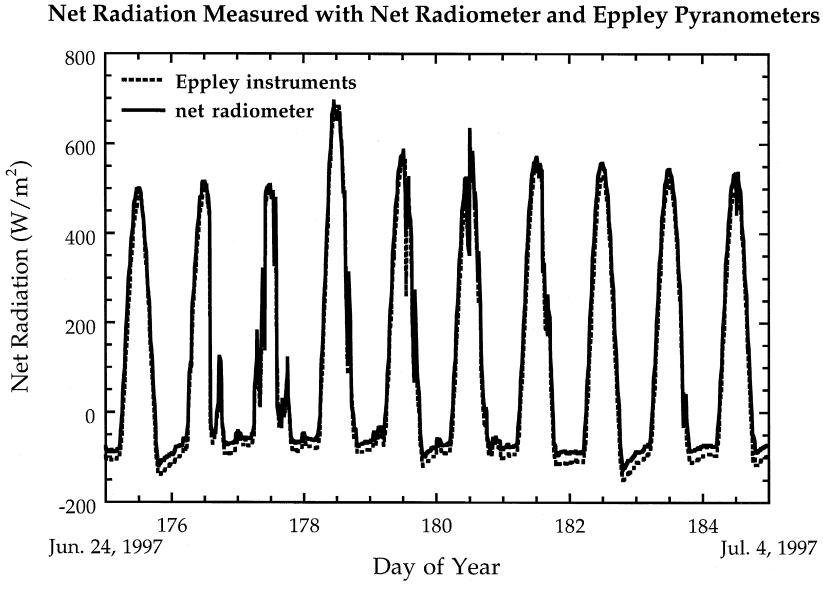

Fig. 4. Comparison of calculated net radiation from the Eppley pyranometers and net radiation measured directly by the REBS Q* 7 modified Fritschen net radiometer at DLW.

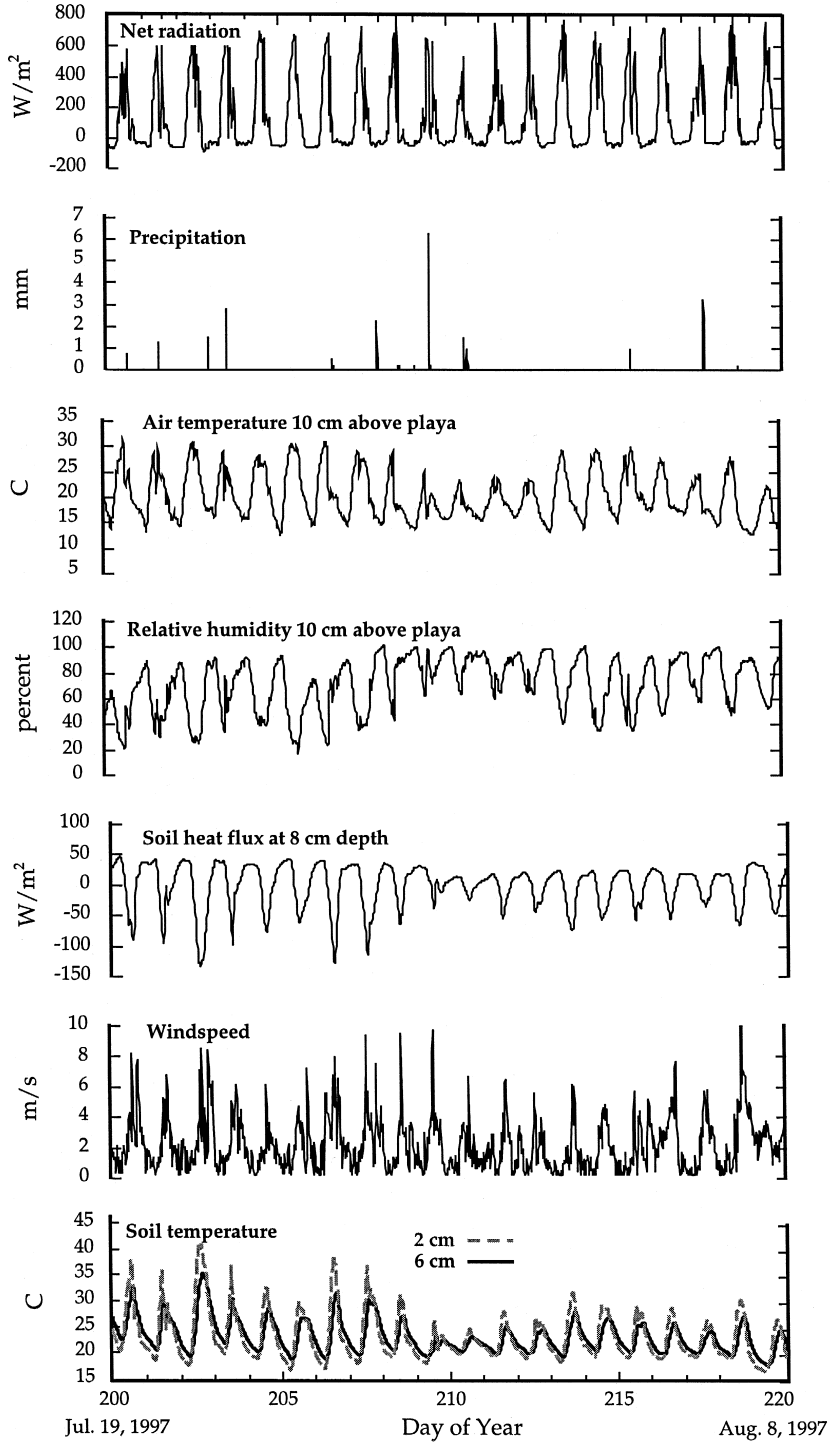

Fig. 5. Selected outputs from the E-12 meteorological station. All variables except precipitation show strong diurnal fluctuations, with soil temperature and heat flux lagging behind the record of air temperature. Precipitation and standing water strongly influence the soil heat flux, soil temperature, and air temperature above the playa.

for comparison to the net radiometer. All sensors are scanned every 30 s by a Campbell Scientific, CR10X data logger powered by a 12 V car battery that is recharged by a solar panel. The data logger stores 20-min averages of the 30-s measurements. The DLW and E-12 stations have been operating continuously since March and May, 1997, respectively. The BENCH station was installed in October, 1997.

Because of the salty environment surrounding the DLW playa station, meteorologic equipment often fails. Salt routinely causes corrosion of electrical contacts in humitter probes and the fans used to aspirate them. Regular maintenance visits have been made to each site to repair and replace equipment. The E-12 and BENCH stations have been much more reliable, requiring infrequent equipment repairs.

7. Results

Maintenance of equipment in the harsh, saline, playa environment presents special problems, and our data sets are often not continuous. They are complete enough, however, to make several observations about evaporation from playa surfaces, as described below and illustrated in Figs. 3–12

7.1. General observations

Records of incoming long- and short-wave energy at DLW show that both exhibit approximately week-long fluctuations related to changes in the synoptic climatology superimposed on a strong seasonal cycle (Fig. 3). No data are recorded after the end of January in 1998 (day 425) because of an electrical fire, which destroyed the datalogger to which the Eppley radiometers and pyranometers were wired. However, the year-long record of calculated net radiation from these instruments compares favorably to measurements of net radiation from the REBS Q^*7 net radiometer over the same time interval, giving us confidence in the net radiation measurements recorded at DLW, as well as those at E-12 and BENCH (Fig. 4). Greatest deviations between the calculated and measured net radiation values at DLW occur at night, when the Eppley instruments routinely return a more negative value of net radiation, a result consistent with the findings of Duell (1990).

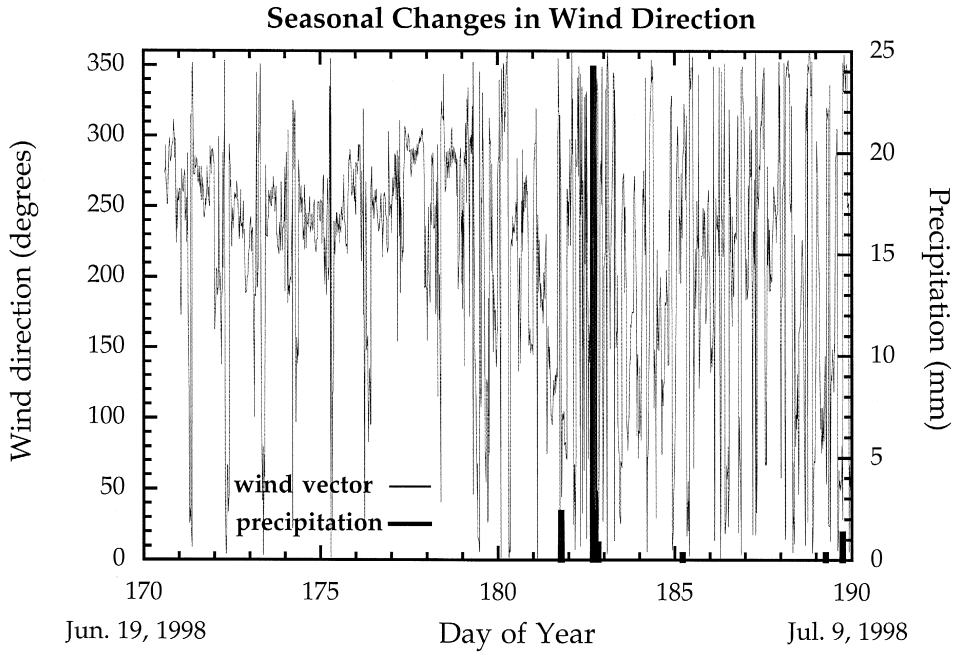

Fig. 6. Changes in wind direction from a very regular pattern of diurnal variations to a much more chaotic pattern mark the beginning of the monsoon season at DLW.

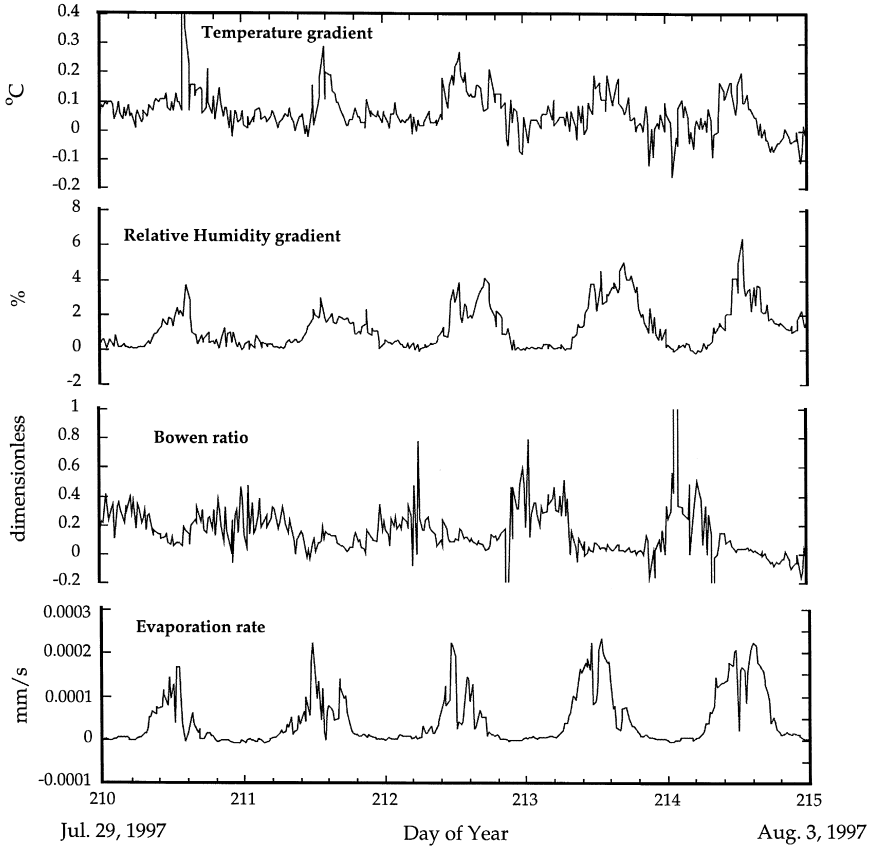

Fig. 7. Evaporation rate depends on the Bowen ratio, which itself is dependent on vertical gradients in temperature and relative humidity. Evaporation rates are highest when values of the Bowen ratio are low. Data are from the E-12 station.

The reasons for the discrepancy are unknown, but it is unlikely to have a large impact on the calculation of evaporation, since most evaporation occurs during the daytime hours.

Like net radiation, air and soil temperature, relative humidity, soil heat flux, and wind speed all show strong diurnal fluctuations. Fig. 5 shows typical sensor output from the E-12 station. Air temperature peaks about 1.5 h after the peak in net radiation, whereas soil heat flux at 8 cm depth peaks about 2.5 h later. Both of these parameters are strongly affected by the presence of water in the playa (compare these quantities to the precipitation graph). When water covers the playa surface, both soil heat flux and air temperature show declines as net radiation previously used to heat the soil and air above it is instead expended in evaporation. A similar response is shown in the soil temperature records.

In winter and spring, winds are predominantly from the west–northwest and reach speeds of 4–10 m/s. At night, winds die down and often shift to a north–northeast direction. In mid-summer, wind directions change dramatically, and exhibit a more chaotic pattern (Fig. 6). The constant directional fluctuations coincide with an increased frequency of precipitation events, marking the development of the Arizona monsoon. Thunderstorms develop over the Estancia Basin nearly every afternoon in the summer, and we have observed wind direction to change repeatedly as one localized updraft dissipates and gives way to another.

7.2. Bowen ratio and evaporation measurements

Like temperature and relative humidity, the Bowen ratio also shows a diurnal cycle, with highest values

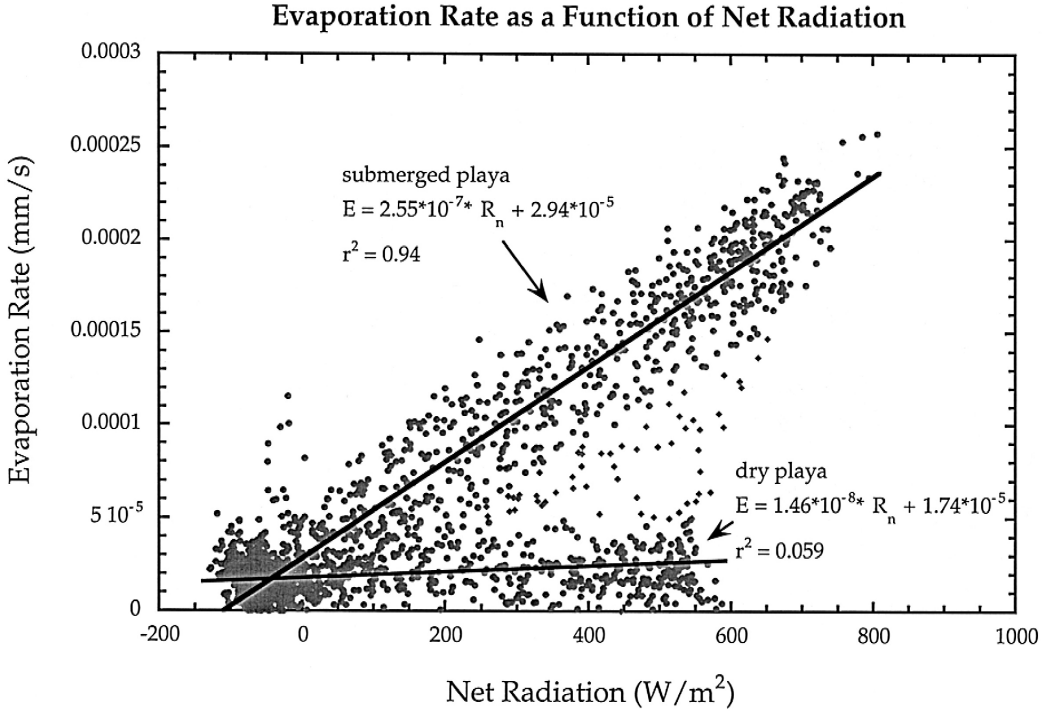

Fig. 8. Evaporation as a function of net radiation at E-12. The data trend with the higher slope likely reflects periods when standing water occupied the playa, whereas the lower trend reflects a lack of standing water. Outliers (diamonds) were not included in the regression equations. E refers to evaporation rate in mm/s; R_n refers to net radiation in W/m^2.

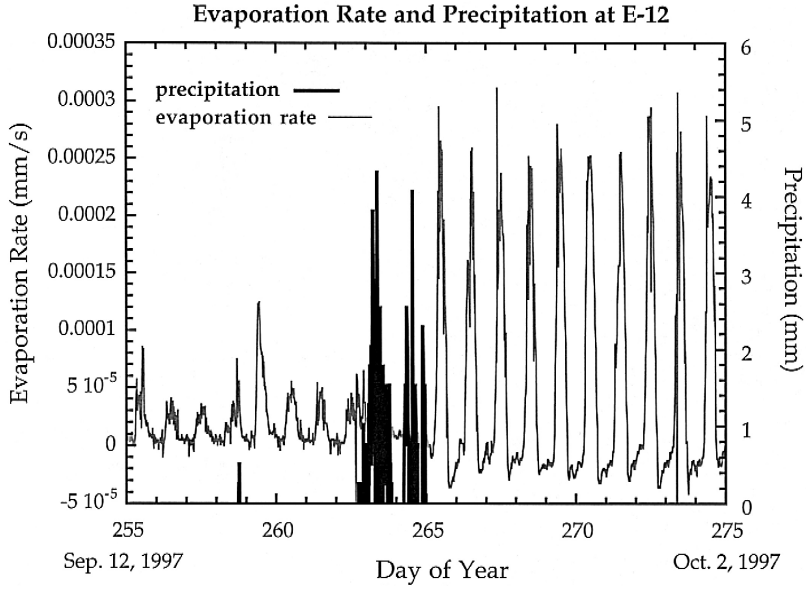

Fig. 9. Evaporation rate and precipitation at E-12 from September 12 through October 2. Evaporation rate increased nearly seven-fold after the storms DOY 262–265 that filled the playa with several centimeters of water.

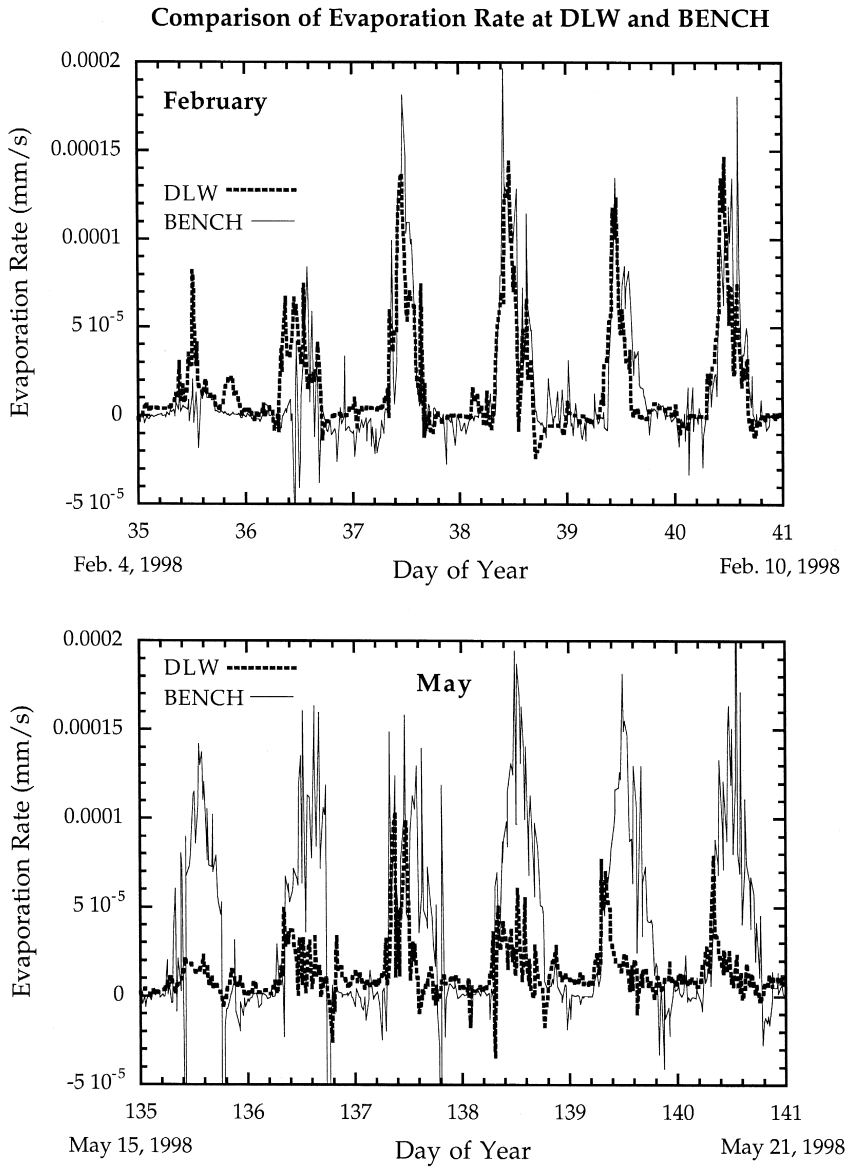

Fig. 10. Comparison of evaporation rate at DLW and BENCH. While comparable to DLW during the winter (February), evaporation rate at BENCH is much greater during the growing season (May).

at night and lowest values during the day (Fig. 7). As windspeeds increase throughout the day, both the vertical temperature and vapor pressure gradients decline. If the temperature gradient collapses entirely, the Bowen ratio achieves a value of 0. If, on the other hand, the vapor pressure gradient collapses, the Bowen ratio achieves nearly infinite positive or negative values. Bowen ratios close to -1 lead to impossibly large values of evaporation (or condensation) rate as the denominator of Eq. (3) approaches zero. For this reason, Bowen ratio values between -0.5 and -1.5 were excluded from evaporation rate calculations, and evaporation at these time periods was calculated from a Bowen ratio created by interpolation between the last and next reasonable values (Malek et al., 1990).

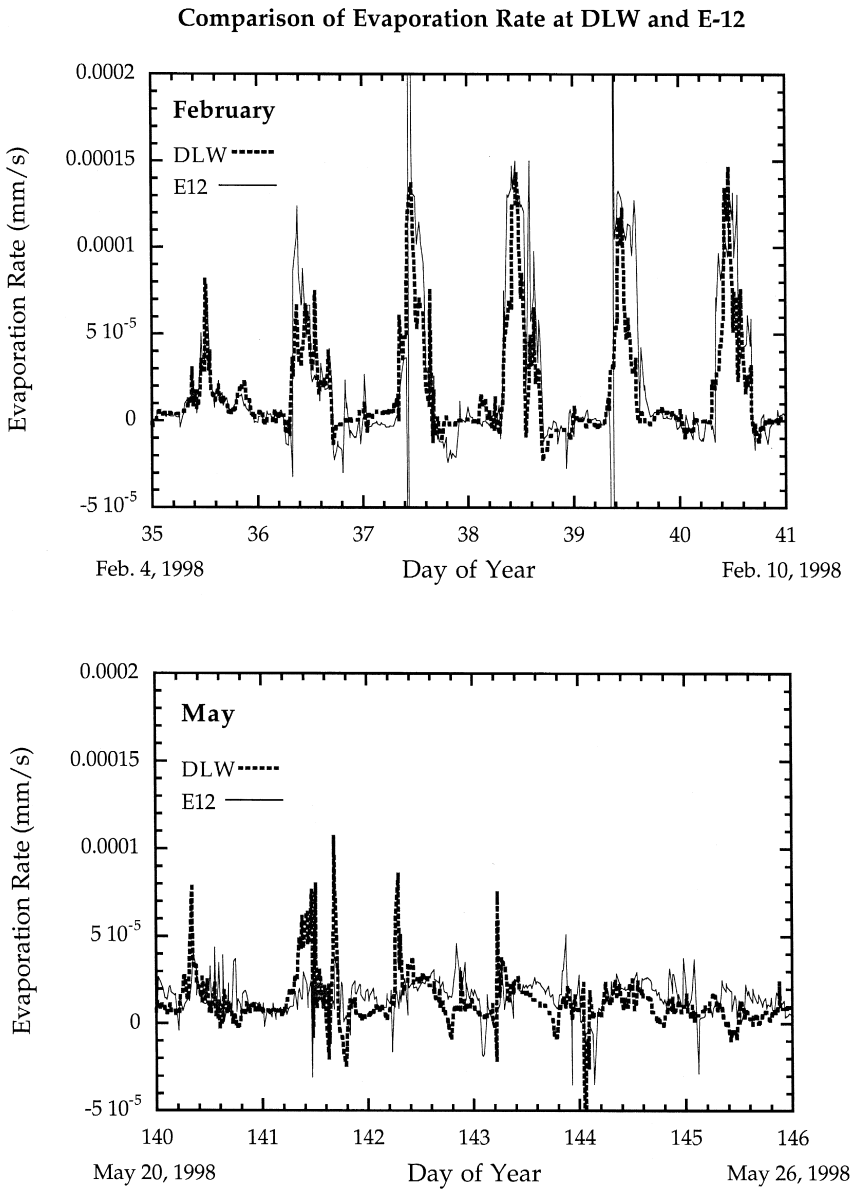

Fig. 11. Comparison of evaporation rate at DLW and E-12. Evaporation rate for the Laguna del Perro playa is similar to that for the E-12 playa regardless of season.

Calculated evaporation rates are highest for low values of the Bowen ratio and are also diurnal (Fig. 7). A small amount of condensation occurs during nighttime hours. Evaporation rate is strongly influenced by net radiation, as can be seen from Eq. (3). Cloudy days, marked by lower than average daytime net radiation values, can cause as much as a 10-fold decline in evaporation rate. A plot of evaporation rate as a function of net radiation confirms the strong relationship between these values but also shows two distinct linear trends (Fig. 8). The upper trend, in which evaporation rate increases with net radiation, is interpreted to represent times when the E-12 playa was submerged. The lower trend, which exhibits a

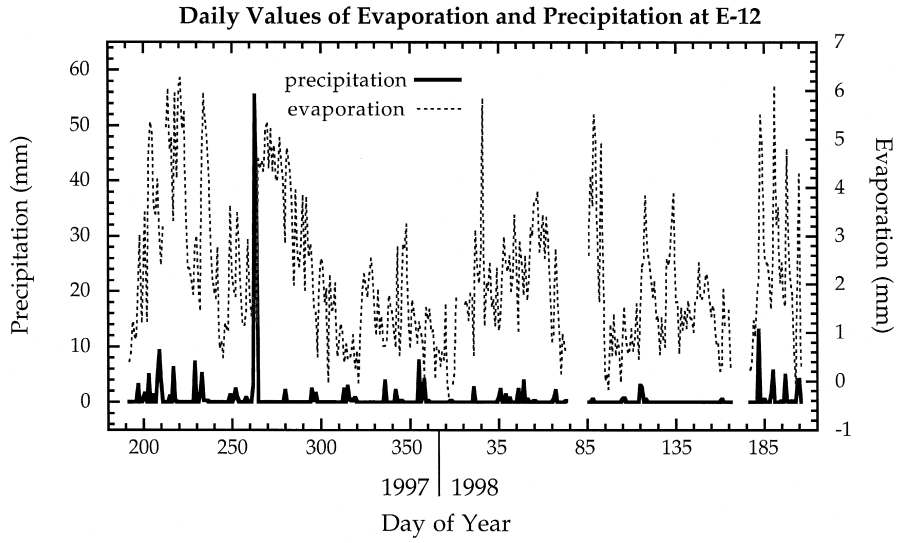

Fig. 12. Daily values of evaporation and precipitation at E-12. Each precipitation event is followed by an increase in evaporation. The storm from day 262–265 (September 19–22) filled the playa with water, causing evaporation rates to remain high into October.

lower slope, represents times when the surface of the playa was dry, and suggests that evaporation rate is fairly constant in the absence of standing water. Fig. 9 confirms the importance of the presence of standing water on evaporation rate. Several centimeters of precipitation fell on the E-12 playa from day of year (DOY) 262–265, resulting in ponded conditions. The day after the storm evaporation rate increased nearly 650% and remained at an elevated level throughout October.

7.3. Comparison among stations

Estimates of evaporation from the Laguna del Perro bench station (BENCH) appear to be comparable to evaporation rates measured on the adjacent playa (DLW) during winter, but very different during the late spring to early summer growing season (Fig. 10). Comparison of data from February and May of 1998 shows that evaporation at BENCH increased markedly as the growing season came on, with daily evaporation peaks increasing both in amplitude and in breadth. In contrast, DLW saw a decline in evaporation rates over the same time interval. This could be related to the transition from evaporation of ponded water on the playa to evaporation from a saturated mud and salt surface.

Data from the two playa stations, DLW and E-12, show that the playas are more similar to each other in their evaporation rates than they are to the vegetated bench. Data from nearly the same time periods as depicted in Fig. 10 show that as evaporation rates declined at DLW, they were matched by nearly equivalent declines at E-12 (Fig. 11). The nearly identical rates of evaporation for these two playas was unexpected because of their different locations within the drainage basin, different water table levels, and their different surface textures, with Laguna del Perro almost perpetually covered with a white crust of halite and other salts, and with the surface of playa E-12 generally a firm, brown mud.

8. Discussion

Daily averages of evaporation and precipitation at E-12 are shown in Fig. 12. As in the case of Fig. 9, which showed the dramatic impact of precipitation on evaporation rate, the daily averages also show that precipitation events are immediately followed by increases in evaporation. Sometimes these increases are short lived and last only a few days. In other instances, amounts of precipitation are sufficiently high to cause elevated levels of evaporation for

weeks. For example, the storm at DOY 262 left enough water in the playa to keep evaporation rates elevated for nearly a month.

DeBrine (1971) determined the amount of groundwater being discharged by playas at the northern end of Estancia Basin. He conducted aquifer pump tests to determine values of transmissivity for the two different valley fill units, the deeper alluvial unit, and a sandy unit within the overlying lacustrine package deposited by Pleistocene Lake Estancia. The transmissivities, combined with water table slope data for the basin, were used to determine a rate of inflow of water into the playas of 71 cm (28 in.)/year. DeBrine (1971) also installed a meteorological station on one of the northern playas to estimate evaporation by several different methods, including the Thornthwaite, Blaney–Criddle, Harbeck–Shjeflo, and pan evaporation methods. He found values that ranged, depending on the technique used, between 69 cm (27.29 in.) and 95 cm (37.29 in.)/year over a 3-year period from 1967–1969.

In the present study, frequent equipment failure at DLW precludes calculation of an annual rate of evaporation, and BENCH has not yet been in operation long enough to acquire an annual record. E-12, however, has functioned reliably for over a year and thus affords us a comparison to DeBrine's estimates of evaporation. Between July 11, 1997 and July 10, 1998, ~27 cm of water fell on the E-12 playa as either rain or snow. During the same time interval, 74 cm of water evaporated. Both precipitation and evaporation may be slightly underestimated due to data losses totaling about 20 days throughout the year (see data breaks in Fig. 12). The value of evaporation compares favorably to the range of values determined by DeBrine. Inasmuch as the DLW and E-12 playas exhibit similar rates of evaporation when DLW is functioning properly, the calculated annual rate of evaporation for DLW may turn out to be nearly the same as that at E-12. The BENCH station will likely show higher annual averages, possibly due to loss of water through transpiration.

Malek et al. (1990) measured evaporation from a playa and adjacent vegetated surface in Pilot Valley, UT between 1986 and 1987. They found a much smaller annual rate of evaporation in this arid setting (22.9 cm), and also noted a nearly three-fold difference in actual evaporation rate between their playa and vegetated sites (the vegetated site measured 63.8 cm). However, their calculated potential evaporation measured 154.3 cm for the playa station and 156.5 cm for the vegetated area, indicating that there simply was not much water available for evaporation. Malek et al. (1990) noted the formation of a salt crust that separated from the underlying playa muds, and thereby increased the resistance of the surface to evaporative loss. While salts form in the Estancia playas, we have never observed them to separate from the underlying muds, and the salts almost always appear saturated or at least damp.

Groundwater discharge playas in Australia give rates of actual evaporation very similar to those found by Malek et al. (1990). Jacobson and Jankowski (1989) used piezometers and a rain gauge to determine an evaporation rate of 27.5 cm/year at Spring Lake in Central Australia. Of this, 22.6 cm/year were attributed to direct precipitation on the playa and 4.9 cm/year to groundwater discharge. These authors note that potential evaporation in the area measures 3 m/year, again showing that greater evaporation would have occurred had water been present. Allison and Barnes (1985) used measurements of deuterium in groundwater at progressively greater depths beneath the playa floor to find a value of evaporation of about 17.0 cm/year at Lake Frome in southern Australia. However, they also report that pan evaporation rates measured as high as 3.2 m/year in this arid region, which receives a scant 10–12.5 cm of precipitation a year. The Estancia estimates of actual evaporation fall well within the range of actual and potential evaporation at the Australian sites.

The results reported here suggest that it will be possible to include meteorological estimates of evaporation from playa surfaces as a component of the basin hydrologic model, which is now being developed. Measurement of water levels in existing and additional piezometers, combined with measurements of transmissivity in lacustrine units, will allow us to independently determine rates of groundwater discharge from the playas. By so doing, we are attempting to separate the volume of water evaporated from groundwater discharge into the playas and from precipitation/surface water components. We believe that such an integrated basin model may allow us to characterize the relationship between meteorological variables and water-table fluctuations

under the present climatic regime. Ultimately, we plan to estimate the changes in hydrologic and meteorological variables associated with the more profound changes in climate during the Holocene and late Pleistocene.

Acknowledgements

National Science Foundation Grant EAR9631538 supported this work. We are thankful to Sue and Mike Harvey for their interest in the project and for allowing us access to remote field areas. We also thank two anonymous reviewers whose comments improved the manuscript.

References

Allen, B.D., 1993. Late Quaternary lacustrine record of paleoclimate, Estancia basin, NM, USA. PhD Thesis, University of New Mexico, Albuquerque, 94 pp.

Allen, B.D., Anderson, R.Y., 1993. Evidence from southwestern North America for rapid shifts in climate during the last glacial maximum. Science 260, 1920–1923.

Allison, G.B., Barnes, C.J., 1985. Estimation of evaporation from the normally ''dry'' Lake Frome in south Australia. Journal of Hydrology 78, 229–242.

Arnold, J.G., Williams, J.R., Maidment, D.R., 1995. Continuous-time water and sediment-routing model for large basins. Journal of Hydraulic Engineering 121 (2), 171–183.

Bachhuber, F.W., 1971. Paleolimnology of Lake Estancia and the Quaternary History of the Estancia Valley, Central New Mexico. PhD Thesis, University of New Mexico, Albuquerque, 238 pp.

Bowen, I.S., 1926. The ratio of heat losses by conduction and by evaporation from any water surface. Physical Review 27, 779–787.

Brutsaert, W.H., 1982. Evaporation into the Atmosphere. Reidel, Boston, 299 pp.

Bryson, R.A., Hare, F.K., 1974. The climates of North America. In: Bryson, R.A., Hare, F.K. (Eds.), World Survey of Climatology vol. 11 Elsevier, New York, pp. 1–47.

Campbell Scientific, 1997. Bowen Ratio Instrumentation Instruction Manual. Campbell Scientific, Logan, UT.

DeBrine, B.E., 1971. Quantitative Hydrologic Study of a Closed Basin with a Playa (Estancia Valley, NM). PhD Thesis, New Mexico Institute of Mining and Technology, Socorro, 165 pp.

Duell, L.F.W., Jr., 1990. Estimates of evapotranspiration in alkaline scrub and meadow communities of Owens Valley, CA, using the Bowen ratio, eddy-correlation, and Penman-combination methods. U.S. Geological Survey Water-Supply Paper 2370.

Fuchs, M., Tanner, C.B., 1968. Calibration and field test of soil heat flux plates. Soil Science Society of America Proceedings 32, 326–328.

Hales, J.E. Jr., 1974. Southwestern United States summer monsoon source-Gulf of Mexico or Pacific Ocean? Journal of Applied Meteorology 13, 331–342.

Hostetler, S.W., 1987. Simulation of lake evaporation with an energy balance-eddy diffusion model of lake temperature: Model development and validation, and application to lake-level variations at Harney–Malheur Lake, OR. PhD Thesis, University of Oregon, Eugene, 162 pp.

Hostetler, S.W., Bartlein, P.J., 1990. Simulation of Lake Evaporation with Application to Modeling Lake Level Variations of Harney–Malheur Lake, OR. Water Resources Research 26, 2603–2612.

Hostetler, S.W., Benson, L.V., 1994. Stable isotopes of oxygen and hydrogen in the Truckee River–Pyramid Lake surface–water system: 2. A predictive model of $\delta^{18}O$ and $\delta^{2}H$ in Pyramid Lake. Limnology and Oceanography 39, 356–364.

Jacobson, G., Jankowski, J., 1989. Groundwater-discharge processes at a central Australian playa. Journal of Hydrology 105, 275–295.

Leopold, L.B., 1951. Pleistocene climate in New Mexico. American Journal of Science 249, 152–168.

Malek, E., Bingham, G.E., McCurdy, G.D., 1990. Evapotranspiration from the margin and moist playa of a closed desert valley. Journal of Hydrology 120, 15–34.

McDonald, M.G., Harbaugh, A.W., 1988. A modular three-dimensional finite-difference ground-water flow model. U.S. Geological Survey Techniques of Water-Resources Investigations TWI 6-A1, 586 pp.

NOAA (National Oceanic and Atmospheric Administration), annual series. Climatological data annual summary, New Mexico. National Climatic Data Center, Asheville, NC.

Oke, T.R., 1987. Boundary Layer Climates. 2nd edn. Routledge, NY, 435 pp.

Titus, F., 1969. Late Tertiary and Quaternary hydrogeology of Estancia Basin, central NM. PhD Thesis, University of New Mexico, Albuquerque, 179 pp.

Tomlinson, S.A., 1996. Evaluating evapotranspiration for six sites in Benton, Spokane, and Yakima Counties, Washington, May 1990 to September 1992. U.S. Geological Survey Water-Resources Investigations Report 96-4002.

Tuan, Y., Everard, C.E., Widdison, J.G., Bennett, I., 1973. The Climate of New Mexico. New Mexico State Planning Office, Santa Fe, 197 pp.

Weaver, H.L., Campbell, G.S., 1985. Use of peltier coolers as soil heat flux transducers. Soil Science Society of America Journal 49, 1065–1067.

Winter, T.C., 1981. Uncertainties in estimating the water balance of lakes. Water Resources Bulletin 17, 82–115.